2001；345：1740-1746
5) 神田直昭，矢坂正弘，大坪亮一，他：虚血性脳血管障害における右左シャントおよび心房中隔瘤の意義－コントラスト経食道心エコー図による検討－　臨床神経学 1998；38：213-218
6) 米村公伸，木村和美，長谷川泰弘，他：50歳以下発症の脳梗塞の検討．臨床神経学 2000；40：881-886
7) Gautier JC, Durr A, Koussa S, et al：Paradoxical cerebral embolism with a patent foramen ovale. *Cerebrovasc Dis* 1991；1：193-202
8) 木村和美，橋本洋一郎，石原　明，他：剖検にて卵円孔に紐状血栓が認められた奇異性脳塞栓症の1例．臨床神経学 1994；34：56-60

8. 脳血管障害における メタボリックシンドロームのEBM

横田千晶　峰松一夫

メタボリックシンドロームは，心血管疾患発生の危険度の高い症候群として注目されている．本症候群は，national cholesterol education program's adult treatment panel III report (NCEP-ATP-III)[1,2] より，

1) 腹部肥満
　(ウエスト周囲: 男性＞102cm, 女性＞88cm)
2) 中性脂肪高値（≧150mg/dl）
3) HDLコレステロール低値
　(男性＜40mg/dl，女性＜50mg/dl)
4) 高血圧（≧130/≧85mmHg）
5) 空腹時血糖の高値（≧110mg/dl）

の5つのうち3つ以上を満たしているものと定義されている．本稿では，NCEP-ATP-IIIにて定義されたメタボリックシンドロームと，頸動脈硬化性病変および脳卒中発生に関するEBMにつき概説する．

メタボリックシンドロームの頻度と頸動脈硬化性病変

4つの民族を含む1,276例を対象としたカナダの研究では，メタボリックシンドロームの頻度は全体で25.8%であり，その頻度は民族間で有意に異なっていた（Native Indian: 41.6%，南アジア人: 25.9%，ヨーロッパ人: 22%，中国人: 11%）[3]．頸動脈エコーにより測定された頸動脈壁の内膜と中膜とを合わせた厚さ，すなわち内中膜複合体厚（IMT）の最大値は，メタボリックシンドローム群の平均0.78mmに対して，対照群では0.74mmであり，前者で有意に厚かった．糖尿病非合併例に限っても，メタボリックシンドローム群のIMT最大厚の平均値が有意に厚かった．頸動脈IMTは全身の動脈硬化の程度を表わす指標とされていることから，この結果はメタボリックシンドローム群における動脈硬化の進展を示唆している．さらに，IMT最大厚の平均値が50パーセンタイル以下の群（I群）と50パーセンタイルを超える群（II群）に分けて，各群における性，年齢，喫煙で補正した心血管疾患合併（冠動脈疾患，脳卒中）頻度を比較したところ，II群での合併頻度がI群に比べて有意に高く，特にメタボリックシンドローム群での合併頻度が著しく高かった（図1）．糖尿病非合併例に限っても同様の結果であった．本研究では，メタボリックシンドローム群での血中plasminogen activator inhibitor-1値が有意に高かったことから，線容系の異常がメタボリックシンドローム群にみられる動脈硬化の進行，心血管疾患発症と関連するのではないかと考察している．

動脈硬化性疾患を有する1,045例（冠動脈疾患502例，脳卒中236例，閉塞性動脈硬化症218例，腹部大動脈瘤89例）を対象としたオランダの研究では，全体の45%がメタボリックシンドロームを合併していた[4]．脳卒中例におけるメタボリックシンドロームの合併頻度は43%であった．メタボリックシンドローム合併例は，非合併例に比べて有意に両側総頸動脈のIMT平均値が厚かった（0.98mm vs 0.92mm）．

メタボリックシンドロームと脳卒中発生

10,357例を対象とした横断研究Third National Health and Nutrition Examination Surveyにおいて，心筋梗塞または脳卒中例は1,098例（心筋梗塞/脳卒中群），脳卒中例は464例（脳卒中群）

よこた ちあき／国立循環器病センター内科脳血管部門，脳血管障害研究室
みねまつ かずお／同 内科脳血管部門部長

0388-2969/04/¥500/論文/JCLS

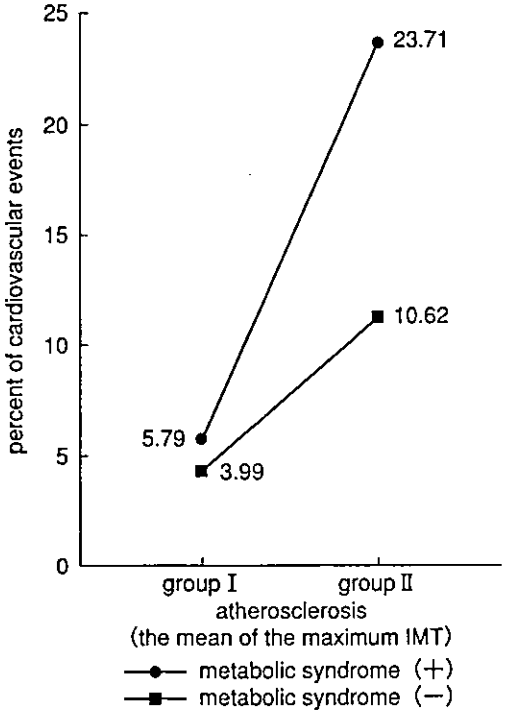

図1　内中膜複合体最大厚別の心血管疾患合併（冠動脈疾患，脳卒中）頻度[3]

I群は，内中膜複合体最大厚の平均値が50パーセンタイル以下，II群は，50パーセンタイルを超える群（II群）を表わす．性，年齢，喫煙で補正した心血管疾患合併頻度は，I群に比べてII群で有意に高かった．
IMT: 内中膜複合体厚．

であった[5]．各群において，メタボリックシンドローム自体が，その他の危険因子と比べてどの程度，心血管疾患と関連しているのか（syndrome model），さらにメタボリックシンドロームを構成する各病態と心血管疾患との関連について（component model）も明らかにするため，ロジスティック回帰分析（年齢，性，人種，喫煙の有無で補正）による検討を行った．メタボリックシンドロームは，いずれの群においても有意な関連因子となっていた（表1）．メタボリックシンドロームを構成する病態の中では，脳卒中群においては高トリグリセリド血症のみが，心筋梗塞/脳卒中群では，高トリグリセリド血症，低HDLコレステロール血症，インスリン抵抗性，高血圧が有意な関連因子であった．

心血管疾患や悪性腫瘍の既往がない健常女性14,719例を8年間にわたり経過観察したwomen's health study（WHS）では，メタボリックシンドローム群では対照群に比較して，有意に有害事象（心筋梗塞，脳卒中，冠動脈再建術，心血管死）発生率が高かった[6]．さらに，これらの有害事象発生予測に高感度CRPの測定がきわめて重要であることが示された．残念ながら，本研究では，脳卒中発生のみについての解析結果は示されていない．

心筋虚血が疑われ，冠動脈造影検査が施行された755例の女性を対象としたwomen's ischemia syndrome evaluation（WISE）studyは，正常群，糖尿病治療歴のないメタボリックシンドローム群，糖尿病治療歴のあるメタボリックシンドローム群の3群を，冠動脈有意狭窄性病変の有無別に4年間経過観察し，有害事象（死亡，心筋梗塞，脳卒中，心不全）発生率につき比較検討した[7]．その結果，有意狭窄性病変例では，正常群に比べて，糖尿病治療の有無にかかわらず，メタボリックシンドローム群での有害事象発生率が有意に高かった．有意狭窄性病変のない例での有害事象発生率には，3群間に有意差はなかった．本研究においても，脳卒中発生のみについての結果は示されていない．

●おわりに

現在までに報告されたメタボリックシンドロームに関する大規模臨床研究は，すべて欧米でなされたものである．これらの研究においても，脳卒中発生を主要エンドポイントとした前向き研究はみあたらない．いまだメタボリックシンドロームと脳卒中との直接的関連に言及した研究は少ないものの，脳卒中発生の危険因子をmultiple risk factorsとして捉え直したFramingham studyの報告は注目される[8]．わが国における代表的疫学研究である久山町研究において，最近30～40年間に耐糖能異常の頻度は2～3倍，高コレステロール血症は6～10倍に急増していることが示されている[9]．わが国の脳梗塞急性期患者14,864例を検討した研究（J-MUSIC）でも，糖尿病と高脂血症の頻度が高かった関東，近畿，中・四国において，アテローム血栓性脳梗塞が高率であった[10]．わが国におけるメタボリックシンドロームと脳血管障害についてのEBMは，まさに今後の課題で

表1 メタボリックシンドロームと心筋梗塞/脳卒中との関連[5]

	心筋梗塞または脳卒中			脳卒中		
	OR	95%CI	p value	OR	95%CI	p value
syndrome model						
metabolic syndrome	2.05	1.64～2.57	＜0.0001	2.16	1.48～3.16	0.0002
人種 (vs non-Hispanic white)						
non-Hispanic black	1.36	1.06～1.76	0.0177	1.49	1.03～2.17	0.0358
Mexican-American	0.81	0.56～1.18	0.2681	0.91	0.58～1.42	0.6746
Other	1.44	0.71～2.92	0.2996	2.11	0.94～4.74	0.0704
喫煙 現在	2.17	1.49～3.14	0.0001	2.13	1.36～3.32	0.0013
過去	1.60	1.24～2.07	0.0006	1.35	0.90～2.04	0.1428
年齢	1.08	1.07～1.09	＜0.0001	1.08	1.06～1.09	＜0.0001
性 (女性/男性)	0.48	0.38～0.61	＜0.0001	0.94	0.65～1.38	0.7667
Component model						
Syndrome components						
腹部肥満	1.11	0.88～1.42	0.3719	0.97	0.58～1.64	0.9154
高TG血症	1.66	1.20～2.30	0.0030	1.87	1.22～2.87	0.0052
低HDL-C血症	1.35	1.05～1.74	0.0199	1.18	0.73～1.90	0.5012
高血圧症	1.44	1.00～2.08	0.0510	1.56	0.94～2.59	0.0827
インスリン抵抗性	1.30	1.03～1.66	0.0298	1.36	0.93～1.98	0.1119

OR: Odds ratio, CI: Confidence interval, TG: トリグリセリド, HDL-C: HDLコレステロール (by logistic regression model).

いえよう.

文 献

1) Third report of the National Cholesterol Education Program (NCEP) expert panel on detection, evaluation, and treatment of high blood cholesterol in adults (Adult Treatment Panel III). Final report. Circulation 2002; 106: 3143–421.
2) Grundy SM, Brewer HB, Cleeman JI, et al. Definition of metabolic syndrome: Report of the National Heart, Lung, and Blood Institute/American Heart Association conference on scientific issues related to definition. Circulation 2004; 109: 433–8.
3) Anand S, Yi Q, Gerstein H, et al. Relationship of metabolic syndrome and fibrinolytic dysfunction to cardiovascular disease. Circulation 2003; 108: 420–5.
4) Olijhoek JK, van der Graaf Y, Banga JD, et al. The metabolic syndrome is associated with advanced vascular damage in patients with coronary heart disease, stroke, peripheral arterial disease or abdominal aortic aneurysm. Eur Heart J 2004; 25: 342–8.
5) Ninomiya JK, L'Italien G, Criqui MH, et al. Association of the metabolic syndrome with history of myocardial infarction and stroke in the Third National Health and Nutrition Examination Survey. Circulation 2004; 109: 42–6.
6) Ridker PM, Buring JE, Cook NR, et al. C-reactive protein, the metabolic syndrome, and risk of incident cardiovascular events: An 8-year follow-up of 14 719 initially healthy American women. Circulation 2003; 107: 391–7.
7) Marroquin OC, Kip KE, Kelley DE, et al. Metabolic syndrome modifies the cardiovascular risk associated with angiographic coronary artery disease in women: A report from the Women's Ischemia Syndrome Evaluation. Circulation 2004; 109: 714–21.
8) Wolf PA, D'Agostino RB, Belanger AJ, et al. Probability of stroke: A risk profile from the Framingham study. Stroke 1991; 22: 312–8.
9) Ohmura T, Ueda K, Kiyohara Y, et al. Prevalence of type 2 (non-insulin-dependent) diabetes mellitus and impaired glucose tolerance in the Japanese general population: The Hisayama study. Diabetologia 1993; 36: 1198–203.
10) 数井誠司, 木村和美, 峰松一夫, 他. 急性期脳梗塞の臨床像およびその医療の地域差に関する多施設共同研究. 臨床神経 2002; 42: 736–44.

Available online at www.sciencedirect.com

SCIENCE DIRECT

Molecular Brain Research 126 (2004) 114–120

MOLECULAR BRAIN RESEARCH

www.elsevier.com/locate/molbrainres

Research report

Calcium influx pathways in rat CNS pericytes

Masahiro Kamouchi*, Takanari Kitazono, Tetsuro Ago, Masanori Wakisaka, Hiroaki Ooboshi, Setsuro Ibayashi, Mitsuo Iida

Department of Medicine and Clinical Science, Graduate School of Medical Sciences, Kyushu University, Maidashi 3-1-1, Higashi, Fukuoka 812-8582, Japan

Accepted 25 March 2004
Available online 4 May 2004

Abstract

In central nervous system (CNS), pericytes have been proposed to play a role in broad functional activities including blood–brain barrier, microcirculation, and macrophage activity. However, contractile responses and Ca^{2+} signaling in CNS pericytes have not been elucidated. The aim of the present study is to investigate contractility and Ca^{2+} influx pathway in CNS pericytes. CNS pericytes were cultured from rat brain. Contraction of the pericytes in response to various stimuli was evaluated by the change in surface area measured by a light microscope with a digital camera. Reverse transcription and polymerase chain reaction (RT–PCR) was performed to examine the expression of mRNA of α-smooth muscle actin. Intracellular Ca^{2+} was measured using fura-2 fluorescence spectroscopy. A23187 (Ca^{2+} ionophore), high external K^+ (4×10^{-2} mol/l), endothelin-1, and serotonin induced contraction of CNS pericytes. RT–PCR analysis revealed the expression of α-smooth muscle actin in CNS pericytes. Cytosolic Ca^{2+} ($[Ca^{2+}]i$) increased after application of high concentration of external K^+, tetraethylammonium, and charybdotoxin, which was inhibited by nicardipine and removal of external Ca^{2+}. Angiotensin-II, serotonin, acetylcholine, ATP, and endothelin-1 caused biphasic response in $[Ca^{2+}]i$. In response to these agents, $[Ca^{2+}]i$ rapidly increased and then decayed to a relatively constant Ca^{2+} plateau. The Ca^{2+} plateau was partially inhibited by nicardipine and completely abolished by omission of external Ca^{2+}. After intracellular Ca^{2+} store was depleted by the removal of external Ca^{2+} and addition of thapsigargin, reapplication of external Ca^{2+} evoked increases in $[Ca^{2+}]i$. These results indicate that CNS pericytes express mRNA of α-smooth muscle actin and possess contractile ability. In CNS pericytes, resting membrane potential is regulated by large conductance Ca^{2+}-activated K^+ channels and Ca^{2+} enters into the cells via L-type voltage-dependent Ca^{2+} channels, agonist-activated Ca^{2+} permeable channels, and capacitative Ca^{2+} entry pathways.

Theme: Other systems of the CNS
Topic: Brain metabolism and blood flow

Keywords: Cerebrovascular circulation; Capillaries; Calcium channel; Calcium signaling

1. Introduction

Pericytes are cells of the vasculature associated with microvessels such as arterioles, venules, and particularly capillaries [1,10,28]. The pericytes appear to be embedded in the basement membrane of the blood vessels and have an important role in the regulation of the vascular functions. Especially, the pericytes closely interact with vascular endothelial cells and is thereby proposed to modulate the functions of the endothelial cells. It is reported that the pericytes modulate the growth and development of the endothelial cells induced by several growth factors, i.e. transforming growth factor-β-1 [2,36], basic fibroblast growth factor [34], and vascular endothelial growth factor [17]. Effects of the pericytes on the endothelial cells are complicated and may be mediated by direct contact and/or production of extracellular matrix components [29]. Moreover, it is also shown that the pericytes have functions of macrophage [32]. Thus, the pericytes may have an important role in the regulation of vascular development and mature microvessel integrity [19,20,28] and may also participate in the immune responses [32].

* Corresponding author. Tel.: +81-92-642-5256; fax: +81-92-642-5271.
E-mail address: kamouchi@intmed2.med.kyushu-u.ac.jp (M. Kamouchi).

0169-328X/$ - see front matter © 2004 Elsevier B.V. All rights reserved.
doi:10.1016/j.molbrainres.2004.03.008

In the central nervous system (CNS), the pericyte has an oval or oblong cell body extending several primary processes which encircle the blood vessels [28,32]. The endothelial cells in CNS have highly specific properties compared with non-cerebral blood vessels, i.e. maintenance of blood–brain barrier and regulation of the cerebral blood flow [8,21]. Because CNS pericytes also contact closely with the endothelial cells, the pericytes may have an important role in such specific properties of the cerebrovascular endothelial cells [1,8,21,32].

It has been assumed that the pericytes have contractile ability as smooth muscle cells in the large blood vessels, since the pericytes appear to reside on the microvasculature where there is little or no smooth muscle. Contractile response of CNS pericytes may be important in the maintenance of the blood–brain barrier. However, there are no studies so far to investigate the contractile response of CNS pericytes. Moreover, little has been known concerning Ca^{2+} signaling in CNS pericytes. In the present study, we isolated CNS pericytes from the brain capillaries and investigated the contractility and Ca^{2+} influx pathways of the cells.

2. Materials and methods

2.1. Cell culture

Male Sprague–Dawley rats (5 weeks old) were anaesthetized with pentobarbital and were decapitated. Brain was homogenized and filtered through a sieve of 85-μm pore size. The capillaries where there is no smooth muscle trapped at the thieve were isolated and incubated at 37 °C in Dulbecco's modified Eagle's medium (DMEM) supplemented with 10% fetal bovine serum (Sigma). After a few days, colonies of pericytes with characteristic shape (Fig. 1) proliferated from each capillary. After the capillary was removed, the primary pericyte colonies were gently scraped and subcultured in other dishes. CNS pericytes were identified by their morphological characteristics [33] and the absence of immunostaining for von Willebrand factor and uptake of dil-LDL. The cells from third to fifth passages were used for the experiments. Morphological feature and pharmacological responses to various vasoactive agents were preserved throughout all the passage (data not shown).

2.2. Reverse transcription and polymerase chain reaction (RT–PCR)

Total RNAs from the cultured pericytes were prepared with TRIzol reagent (Invitrogen). One microgram of total RNA was reverse transcribed by AMV-transcriptase (Roche) in a total volume of 20 μl. Using 1 μl of the product as a template, PCR was performed with primers specific for rat smooth muscle α-actin (forward; 5′-GTGACTCACAACGTGCCTAT-3′, reverse; 5′-TTAGAAGCATTTGCGGTGGA-3′). After preincubation at 94 °C for 5 min, PCR was performed with 30 cycles of denaturation at 94 °C for 10 s, annealing at 58 °C for 10 s, and elongation at 72 °C for 15 s. The PCR products (654 base pairs) were subjected to 1.2% agarose-gel electrophoresis and stained with ethidium bromide. PCR products were sequenced to confirm their identities.

2.3. Contraction experiments

Changes in the tonus of CNS pericytes were examined by measuring surface area according to the method described previously [33]. Briefly, the pericytes were preincubated in HEPES-buffered saline (pH 7.4) of the following composition (in mmol/l): 132.0 $NaCl_2$, 5.9 KCl, 1.2 $MgCl_2$, 1.5 $CaCl_2$, 11.5 glucose, 11.5 HEPES, 1.2 NaH_2PO_4. The cells were examined by a light microscope equipped with a digital camera (Nikon). The margin of the cells was traced and the area within the trace was measured using NIH image (written by W. Rasband). Changes in the surface area were calculated in response to various stimuli. More than 30 cells were used for calculation of surface area. We performed preliminary experiments concerning dose–response relationship and used submaximal to maximal dose of each agonist.

2.4. $[Ca^{2+}]i$ measurement

For the measurement of intracellular Ca^{2+} concentration ($[Ca^{2+}]i$), the fluorescent Ca^{2+} indicator, fura-2, was used. The fura-2 loaded cells were perfused with HEPES-buffered saline and illuminated alternatively at wavelengths of 340 and 380 nm through a rotating filter wheel. The

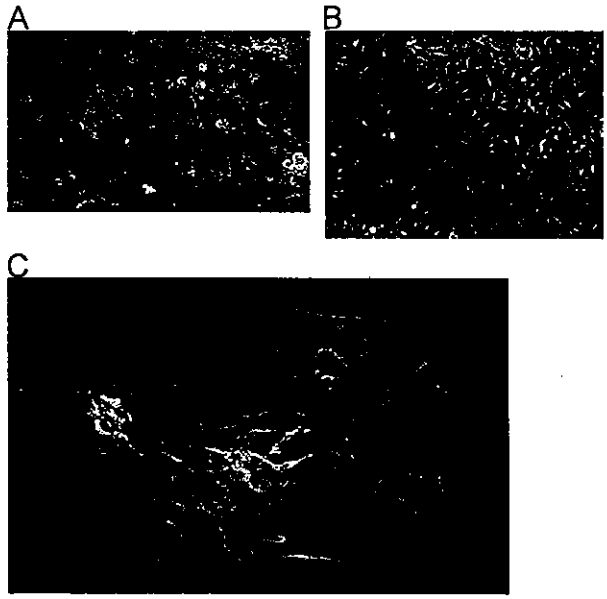

Fig. 1. CNS pericytes. A microscopic feature of cultured CNS pericytes (A, and C) in comparison with basilar arterial endothelial cells (B).

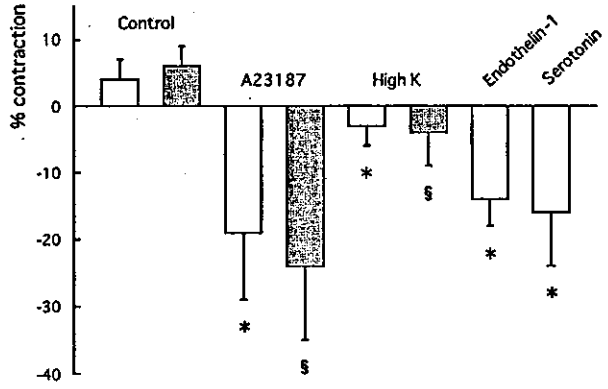

Fig. 2. Contractile responses of CNS pericytes. The surface area of CNS pericytes was measured after application of each stimulus factor. Cells were treated with A23187 (10^{-6} mol/l), high K^+ (4×10^{-2} mol/l), endothelin-1 (10^{-7} mol/l), and serotonin (10^{-6} mol/l) for 30 (open columns) and 60 min (hatched columns). Contractile responses were expressed as % change of the area compared with the basal values. Negative values indicate the reduction in the surface area. $^*P<0.05$ (unpaired t-test, versus control at 30 min), $^{\S}P<0.05$ (unpaired t-test, versus control at 60 min).

fluorescence at wavelength of 510 nm was measured and ratio of that illuminated at 340 and 380 nm was calculated. For Ca^{2+}-free solution, $CaCl_2$ was omitted and 1 mmol/l EGTA was added. All experiments were performed at room temperature.

2.5. Drugs

A23187, serotonin, tetraethylammonium chloride (TEA), nicardipine, serotonin, acetylcholine, ATP, bradykinin, histamine, thapsigargin, wortomannin and genistein were purchased from Sigma and endothelin-1, charybdotoxin, and angiotensin-II were from Peptide Institute.

2.6. Statistical analysis

Pooled data are given as means ± S.D. N is the number of cells examined. Statistical analysis was done by Student's t-test or ANOVA followed by Scheffe's multiple comparison test. P value less than 0.05 was taken as significant.

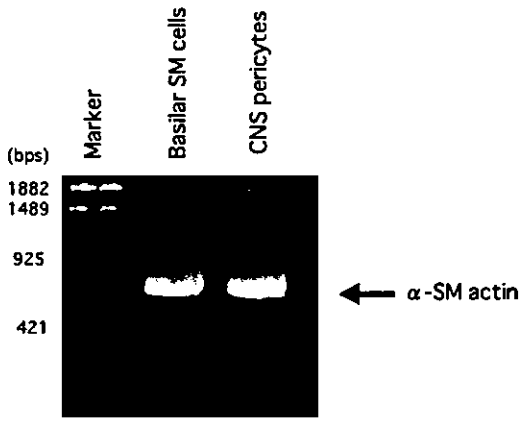

Fig. 3. Expression of α-smooth muscle actin. RT–PCR showed the expression of mRNA of α-smooth muscle actin.

3. Results

3.1. Effects of agonists on the surface area of CNS pericytes

When the cells were incubated with A23187 (Ca^{2+} ionophore), high concentration of external K^+ up to 4×10^{-2} mol/l, endothelin-1 or serotonin, surface area of CNS pericytes was significantly reduced (Fig. 2).

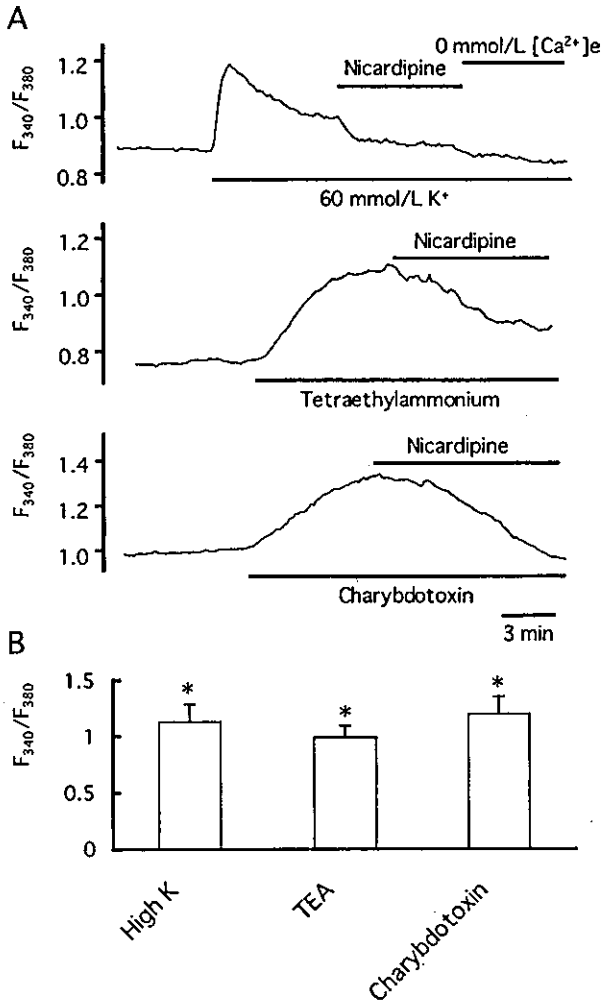

Fig. 4. $[Ca^{2+}]i$ change after depolarizing stimuli. (A) Representative responses of $[Ca^{2+}]i$ in CNS pericytes to membrane depolarization. CNS pericytes were loaded with fura-2 and the fluorescence ratios (F_{340}/F_{380}) were calculated. High concentration of K^+ (6×10^{-2} mol/l), TEA (5×10^{-3} mol/l), charybdotoxin (10^{-7} mol/l), and nicardipine (10^{-6} mol/l) were added in the external solution where indicated. External solution was replaced by Ca^{2+}-free external solution as shown above the traces. (B) Highest peak in $[Ca^{2+}]i$ measured after application of high external K^+ or blockers of K^+ channels. $^*P<0.05$ (paired t-test, versus resting).

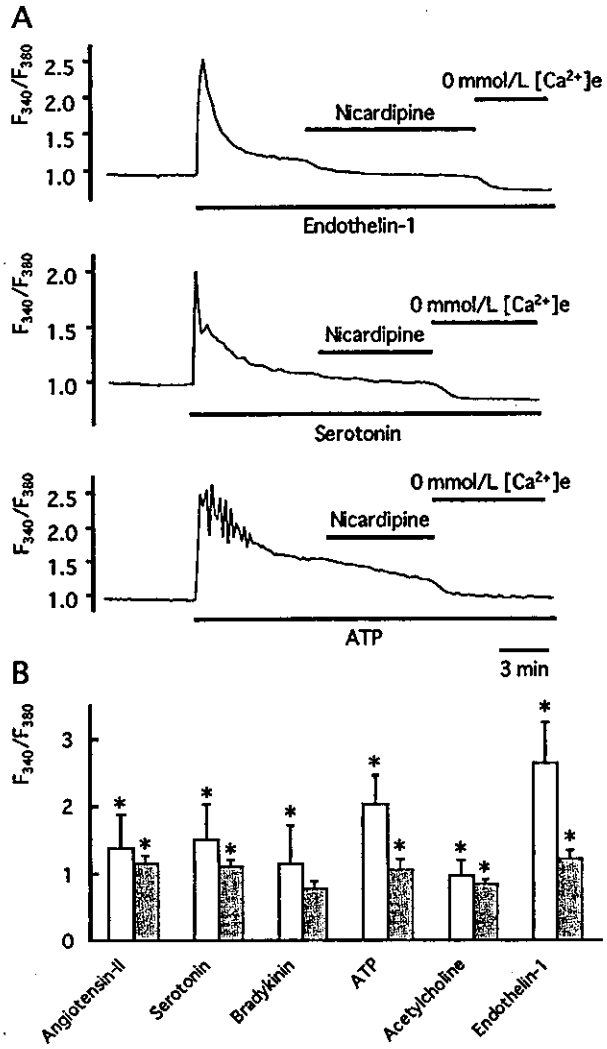

Fig. 5. $[Ca^{2+}]i$ change after vasoactive agonists. (A) Representative responses of $[Ca^{2+}]i$ to vasoactive agonists. Endothelin-1 (10^{-7} mol/l), ATP (5×10^{-5} mol/l), serotonin (3×10^{-5} mol/l), and nicardipine (10^{-6} mol/l) were added in the external solution. (B) Highest peak in $[Ca^{2+}]i$ (open columns) and $[Ca^{2+}]i$ at 8 min (hatched columns) measured after application of various vasoactive agents including angiotensin-II (5×10^{-6} mol/l), serotonin (3×10^{-5} mol/l), bradykinin (5×10^{-6} mol/l), ATP (5×10^{-5} mol/l), acetylcholine (5×10^{-5} mol/l), and endothelin-1 (10^{-7} mol/l). $^{*}P < 0.05$ (paired t-test, versus resting).

3.2. Functional expression of α-smooth muscle actin RNA in CNS pericytes

RT–PCR analysis revealed the expression of the actin RNA in CNS pericytes (Fig. 3).

3.3. Ca^{2+} signaling in CNS pericytes

3.3.1. Involvement of L-type voltage dependent Ca^{2+} channels

After administration of high concentration of external K^{+} solution (6×10^{-2} mol/l), $[Ca^{2+}]i$ increased and then gradually decreased ($n = 45$, Fig. 4A, top; Fig. 4B). Blockade of K^{+} channels by TEA ($n = 10$) or charybdotoxin ($n = 13$) also elicited an increase in $[Ca^{2+}]i$ (Fig. 4A, B). The increase in $[Ca^{2+}]i$ induced by both high K^{+} solution and blockade of K^{+} channels was abolished by removal of external Ca^{2+} or nicardipine (Fig. 4A).

3.3.2. Effects of various agonists

Angiotensin-II ($n = 20$), serotonin ($n = 22$), ATP ($n = 51$), acetylcholine ($n = 12$), and endothelin-1 ($n = 45$) caused a biphasic increase in $[Ca^{2+}]i$. After application of these

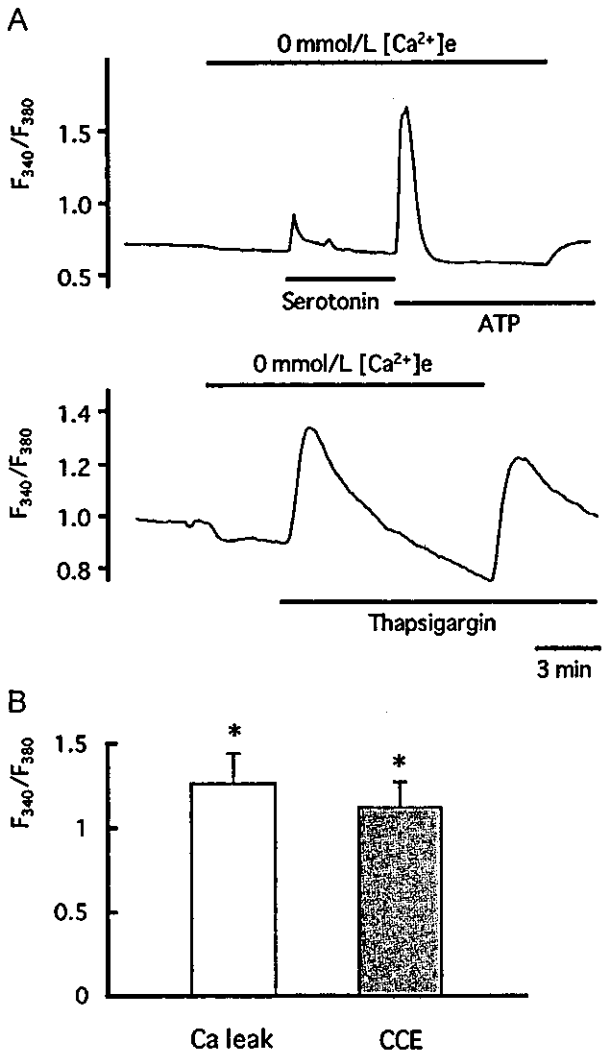

Fig. 6. Capacitative Ca^{2+} entry. (A) Representative responses of $[Ca^{2+}]i$ to depletion of intracellular Ca^{2+} store. Serotonin (3×10^{-5} mol/l), ATP (5×10^{-5} mol/l), and thapsigargin (10^{-6} mol/l) were added in the external solution where indicated. External solution was replaced by Ca^{2+}-free external solution as shown above the traces. (B) Highest peak in $[Ca^{2+}]i$ after application of thapsigargin (10^{-6} mol/l) in the absence of external Ca^{2+} (Ca leak, open column) and that during the re-addition of external Ca^{2+} (capacitative Ca^{2+} entry: CCE, hatched column). $^{*}P < 0.05$ (paired t-test, versus resting).

agonists, $[Ca^{2+}]i$ rapidly increased and then decayed to a relatively constant Ca^{2+} level (Fig. 5A, B). The Ca^{2+} plateau was completely abolished by omission of external Ca^{2+}. After application of bradykinin, $[Ca^{2+}]i$ rapidly increased and decayed to a near resting Ca^{2+} level ($n=11$). Histamine (10^{-4} mol/l, $n=14$) did not induce any change in $[Ca^{2+}]i$. In the absence of external Ca^{2+}, agonists still induced the Ca^{2+} peak (ATP, $n=14$; serotonin, $n=14$), however, the Ca^{2+} plateau was not detected (Fig. 6A). In this condition, reapplication of external Ca^{2+} restored the Ca^{2+} plateau in the pericytes (Fig. 6A).

3.3.3. Mechanisms of agonists-induced Ca^{2+} plateau

Nicardipine attenuated agonist-induced Ca^{2+} plateau, however, did not abolish the Ca^{2+} responses in the pericytes (Fig. 5A). The inhibitory effect of nicardipine on the Ca^{2+} plateau was more prominent in endothelin-1-induced response ($49 \pm 11\%$ inhibition, $n=14$) than ATP-induced response ($38 \pm 14\%$ inhibition, $n=26$; $P<0.05$, unpaired t-test).

After removal of external Ca^{2+}, thapsigargin, an inhibitor of sarco/endoplasmic reticulum Ca^{2+} ATPase, was added in the bath. Thapsigargin evoked a transient $[Ca^{2+}]i$ increase in Ca^{2+}-free solution due to the Ca^{2+} leak from intracellular store sites (Fig. 6A). After depletion of Ca^{2+} store by thapsigargin, application of extracellular Ca^{2+} induced an increase in $[Ca^{2+}]i$ ($n=23$, Fig. 6A, B).

3.3.4. Regulation of Ca^{2+} plateau by signal transduction pathway

Pretreatment of cells with wortomannin, an inhibitor of phosphatidylinositol 3-kinase, for 20 min did not affect the time course of Ca^{2+} decay ($n=15$). On the other hand, $[Ca^{2+}]i$ decayed more rapidly when the cells were pretreated with genistein, an inhibitor of tyrosine kinase, for 20 min ($n=11$). Ca^{2+} plateau and time integral of $[Ca^{2+}]i$ during 10 min were smaller than control in the presence of genistein, although Ca^{2+} peak was not changed (Fig. 7).

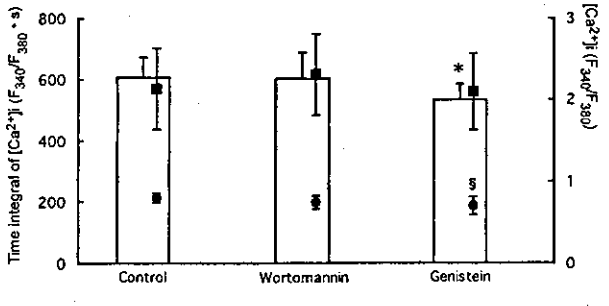

Fig. 7. Regulation of ATP-induced Ca^{2+} influx. After cells were incubated with wortomannin (10^{-7} mol/l) or genistein (2×10^{-4} mol/l) for 20 min, Ca^{2+} peak (closed squares) and Ca^{2+} plateau at 10 min (closed circles) were compared with those of control. Time integral of ratio was also calculated (open columns) and compared among the groups. $^{*}P<0.05$ (ANOVA, Scheffe, versus control, wortomannin), $^{\S}P<0.005$ (ANOVA, Scheffe, versus control).

4. Discussion

4.1. Contractile activity of CNS pericytes

Although several reports have suggested that non-CNS pericytes may have contractile ability, it is still unclear whether CNS pericytes also have contractility in response to vasoactive stimuli [1,4,7,10,16,24,28,30]. In the present study, A23187, a Ca^{2+} ionophore, produced marked contraction of CNS pericytes. Moreover, we found, using RT–PCR, that CNS pericytes expressed α-smooth muscle actin, which is identical to the actin of basilar arterial smooth muscle. The findings suggest that CNS pericytes have a capacity to contract in response to intracellular Ca^{2+} increase, which would be expected since they appear to be oligopotential and function as phagocytes as well as smooth muscle cells. However, it still needs cautions to interpret the results by extrapolating from in vitro observation to the in vivo state.

4.2. Ca^{2+} influx pathways in CNS pericytes

4.2.1. Functional expression of voltage-gated Ca^{2+} channels

As cell population of the vasculature, three types of cells, including smooth muscle cells, endothelial cells, and pericytes are present. Pericytes appear to be the microvessel equivalent of the large vessel smooth muscle [1,10,28,32]. In smooth muscle cells, L-type Ca^{2+} channels mediate depolarization-induced influx of Ca^{2+} into the cells and thus trigger vascular contraction [22]. On the other hand, endothelial cells are nonexcitable and voltage-gated Ca^{2+} channels are not expressed in both cultured and freshly isolated vascular endothelial cells [25,26]. In the present study, the depolarization-induced Ca^{2+} influx is blocked by nicardipine, suggesting that the Ca^{2+} influx may be mediated through activation of voltage-gated Ca^{2+} channels. Moreover, Ca^{2+} increase caused by K^+ channel inhibitors was also blocked by nicardipine. These results suggest that voltage-gated Ca^{2+} channels may play an important role in regulating $[Ca^{2+}]i$ in CNS pericytes.

In cerebral arterial smooth muscle cells, membrane potential is regulated by various ionic conductance including K^+ channels and Cl^- channels which affect the open probability of voltage-gated Ca^{2+} channels [11,15,23]. When $[Ca^{2+}]i$ is increased by various stimuli, both Ca^{2+}-dependent K^+ channels and Cl^- channels are activated and regulate membrane potential, which contributes to the modulation of Ca^{2+} influx [11,12]. As mentioned above, selective blockade of large conductance Ca^{2+}-activated K^+ channels induced Ca^{2+} influx through voltage-gated Ca^{2+} channels in CNS pericytes. Thus, resting membrane potential in the pericytes may be dominated mainly by large conductance Ca^{2+}-activated K^+ channels.

4.2.2. Properties of agonist-induced Ca^{2+} influx

Various vasoactive agents which have been proposed to be involved in pericyte functions were tested to elucidate whether they exert their actions through change in $[Ca^{2+}]i$ [1,5,6,10,16,28,32,35]. In the present study, various agonists evoked a biphasic response in $[Ca^{2+}]i$, although histamine did not produce any significant change in $[Ca^{2+}]i$. Initial peak was independent of extracellular Ca^{2+}, however, the following Ca^{2+} plateau was completely abolished in Ca^{2+}-free medium, suggesting that this phase may be composed of Ca^{2+} influx through Ca^{2+} permeable channels.

In smooth muscle cells, agonists activate Ca^{2+} entry via receptor operated nonselective cation channels which contribute to Ca^{2+} entry in both direct and indirect ways in this cell type [22]. In the endothelial cells, various receptor-activated cation channels gated by binding of agonists to the membrane receptor have been described [25,26], and Ca^{2+} permeable nonselective cation channels presumably play a central role in the Ca^{2+} influx pathway [13,14]. In CNS pericytes, the Ca^{2+} plateau was partially inhibited by dihydropyridine, indicating that the Ca^{2+} plateau may be in part composed of Ca^{2+} influx via voltage-gated Ca^{2+} channels. It is possible that the activation of nonselective cation channels leads to membrane depolarization and thereby causes activation of voltage-gated Ca^{2+} channels. It is also reported that neurotransmitters and other messengers are directly linked to voltage-gated Ca^{2+} channels in smooth muscle cells [3]. The degree of the inhibition by nicardipine was different in each agonist-induced response. Each agonist may differently act on the channels through these two manners.

Ca^{2+} influx may also be controlled by the filling state of $[Ca^{2+}]i$ stores in many non-excitable cells [27]. However, in excitable cells such as smooth muscle cell, the role of capacitative Ca^{2+} entry is less clear [9]. In the present study, we have shown that Ca^{2+} influx pathway through capacitative Ca^{2+} entry mechanism may also exist in CNS pericytes. Capacitative Ca^{2+} entry may be involved in Ca^{2+} influx during agonist stimulation in CNS pericytes.

We demonstrated that genistein, an inhibitor of tyrosine kinase, markedly attenuated acetylcholine-induced Ca^{2+} influx to the cerebral arterial endothelial cells [18]. Moreover, recent reports have suggested the involvement of phosphatidylinositol-3 kinase in the regulation of L-type Ca^{2+} channels [31]. In the present study, the agonist-induced Ca^{2+} plateau was attenuated by genistein but was not affected by wortomannin. These results suggest that the agonist-induced Ca^{2+} influx is subject to the regulation by tyrosine kinase and the activity of phosphatidylinositol-3 kinase may not be closely related to the regulation of Ca^{2+} influx in CNS pericytes.

4.3. Clinical implication

Physiological as well as pathological roles of CNS pericytes are not fully understood. CNS pericytes appear to be important for the transport across the blood–brain barrier and the regulation of vascular permeability [28,32]. The possible role of the pericytes in the regulation of microcirculation and interaction with the endothelial cells is also suggested [10,28]. Moreover, an important role of the pericytes in pathology, and neuropathology in particular, has been indicated in hypertension, diabetic retinopathy, Alzheimer's disease, multiple sclerosis, and CNS tumor formation [1,10]. Because Ca^{2+} is a key intracellular messenger triggering various signaling cascades in CNS pericytes, Ca^{2+} influx pathways in CNS pericytes are considered to become an important candidate for a pharmacological target in the future.

Acknowledgements

This study was supported by Research Grants for Cardiovascular Diseases (11-1) from the Ministry of Health, Labour and Welfare of Japan.

References

[1] G. Allt, J.G. Lawrenson, Pericytes: cell biology and pathology, Cells Tissues Organs 169 (2001) 1–11.
[2] A. Antonelli-Orlidge, K.B. Saunders, S.R. Smith, P.A. D'Amore, An activated form of transforming growth factor β is produced by cocultures of endothelial cells and pericytes, Proc. Natl. Acad. Sci. U. S. A. 86 (1989) 4544–4548.
[3] D.J. Beech, Actions of neurotransmitters and other messengers on Ca^{2+} channels and K^+ channels in smooth muscle cells, Pharmacol. Ther. 73 (1997) 91–119.
[4] R.J. Boado, W.M. Pardridge, Differential expression of α-actin mRNA and immunoreactive protein in brain microvascular pericytes and smooth muscle cells, J. Neurosci. Res. 39 (1994) 430–435.
[5] M.P. Dehouck, P. Vigne, G. Torpier, J.P. Breittmayer, R. Cecchelli, C. Frelin, Endothelin-1 as a mediator of endothelial cell-pericyte interactions in bovine brain capillaries, J. Cereb. Blood Flow Metab. 17 (1997) 464–469.
[6] A.B. Dodge, H.B. Hechtman, D. Shepro, Microvascular endothelial-derived autacoids regulate pericyte contractility, Cell Motil. Cytoskelet. 18 (1991) 180–188.
[7] E. Ehler, G. Karlhuber, H.C. Bauer, A. Draeger, Heterogeneity of smooth muscle-associated proteins in mammalian brain microvasculature, Cell Tissue Res. 279 (1995) 393–403.
[8] A. Frey, B. Meckelein, H. Weiler-Guttler, B. Mockel, R. Flach, H.G. Gassen, Pericytes of the brain microvasculature express γ-glutamyl transpeptidase, Eur. J. Biochem. 202 (1991) 421–429.
[9] A. Gibson, I. McFadzean, P. Wallace, C.P. Wayman, Capacitative Ca^{2+} entry and the regulation of smooth muscle tone, Trends Pharmacol. Sci. 19 (1998) 266–269.
[10] K.K. Hirschi, P.A. D'Amore, Pericytes in the microvasculature, Cardiovasc. Res. 32 (1996) 687–698.
[11] M. Kamouchi, R. Ogata, M. Fujishima, Y. Ito, K. Kitamura, Membrane currents evoked by histamine in rabbit basilar artery, Am. J. Physiol. 272 (1997) H638–H647.
[12] M. Kamouchi, M. Fujishima, Y. Ito, K. Kitamura, Simultaneous activation of Ca^{2+}-dependent K^+ and Cl- currents by various forms of stimulation in the membrane of smooth muscle cells from the rabbit basilar artery, J. Smooth Muscle Res. 34 (1998) 57–68.
[13] M. Kamouchi, A. Mamin, G. Droogmans, B. Nilius, Nonselective

cation channels in endothelial cells derived from human umbilical vein, J. Membr. Biol. 169 (1999) 29–38.
[14] M. Kamouchi, S. Philipp, V. Flockerzi, U. Wissenbach, A. Mamin, L. Raeymaekers, J. Eggermont, G. Droogmans, B. Nilius, Properties of heterologously expressed hTRP3 channels in bovine pulmonary artery endothelial cells, J. Physiol. 518 (Pt. 2) (1999) 345–358.
[15] M. Kamouchi, T. Kitazono, T. Nagao, M. Fujishima, S. Ibayashi, Role of Ca^{2+}-activated K^+ channels in the regulation of basilar arterial tone in spontaneously hypertensive rats, Clin. Exp. Pharmacol. Physiol. 29 (2002) 575–581.
[16] C. Kelley, P. D'Amore, H.B. Hechtman, D. Shepro, Microvascular pericyte contractility in vitro: comparison with other cells of the vascular wall, J. Cell Biol. 104 (1987) 483–490.
[17] Y. Kim, R.Y. Imdad, A.H. Stephenson, R.S. Sprague, A.J. Lonigro, Vascular endothelial growth factor mRNA in pericytes is upregulated by phorbol myristate acetate, Hypertension 31 (1998) 511–515.
[18] J. Kitayama, T. Kitazono, S. Ibayashi, M. Wakisaka, Y. Watanabe, M. Kamouchi, T. Nagao, M. Fujishima, Role of phosphatidylinositol 3-kinase in acetylcholine-induced dilatation of rat basilar artery, Stroke 31 (2000) 2487–2493.
[19] M. Klagsbrun, Regulators of angiogenesis: stimulators, inhibitors, and extracellular matrix, J. Cell. Biochem. 47 (1991) 199–200.
[20] M. Klagsbrun, P.A. D'Amore, Regulators of angiogenesis, Annu. Rev. Physiol. 53 (1991) 217–239.
[21] J. Kunz, D. Krause, J. Gehrmann, R. Dermietzel, Changes in the expression pattern of blood–brain barrier-associated pericytic aminopeptidase N (pAP N) in the course of acute experimental autoimmune encephalomyelitis, J. Neuroimmunol. 59 (1995) 41–55.
[22] H. Kuriyama, K. Kitamura, T. Itoh, R. Inoue, Physiological features of visceral smooth muscle cells, with special reference to receptors and ion channels, Physiol. Rev. 78 (1998) 811–920.
[23] T. Nagao, S. Ibayashi, S. Sadoshima, K. Fujii, Y. Ohya, M. Fujishima, Distribution and physiological roles of ATP-sensitive K^+ channels in the vertebrobasilar system of the rabbit, Circ. Res. 78 (1996) 238–243.
[24] V. Nehls, D. Drenckhahn, Heterogeneity of microvascular pericytes for smooth muscle type α-actin, J. Cell Biol. 113 (1991) 147–154.
[25] B. Nilius, G. Droogmans, Ion channels and their functional role in vascular endothelium, Physiol. Rev. 81 (2001) 1415–1459.
[26] B. Nilius, F. Viana, G. Droogmans, Ion channels in vascular endothelium, Annu. Rev. Physiol. 59 (1997) 145–170.
[27] A.B. Parekh, R. Penner, Store depletion and calcium influx, Physiol. Rev. 77 (1997) 901–930.
[28] H.K. Rucker, H.J. Wynder, W.E. Thomas, Cellular mechanisms of CNS pericytes, Brain Res. Bull. 51 (2000) 363–369.
[29] A.M. Schor, A.E. Canfield, P. Sloan, S.L. Schor, Differentiation of pericytes in culture is accompanied by changes in the extracellular matrix, In Vitro Cell. Dev. Biol. 27A (1991) 651–659.
[30] D. Shepro, N.M. Morel, Pericyte physiology, FASEB J. 7 (1993) 1031–1038.
[31] S.F. Steinberg, PI3King the L-type calcium channel activation mechanism, Circ. Res. 89 (2001) 641–644.
[32] W.E. Thomas, Brain macrophages: on the role of pericytes and perivascular cells, Brain Res. Brain Res. Rev. 31 (1999) 42–57.
[33] M. Wakisaka, T. Kitazono, M. Kato, U. Nakamura, M. Yoshioka, Y. Uchizono, M. Yoshinari, Sodium-coupled glucose transporter as a functional glucose sensor of retinal microvascular circulation, Circ. Res. 88 (2001) 1183–1188.
[34] S. Watanabe, N. Morisaki, M. Tezuka, K. Fukuda, S. Ueda, N. Koyama, K. Yokote, T. Kanzaki, S. Yoshida, Y. Saito, Cultured retinal pericytes stimulate in vitro angiogenesis of endothelial cells through secretion of a fibroblast growth factor-like molecule, Atherosclerosis 130 (1997) 101–107.
[35] S. Yamagishi, C.C. Hsu, K. Kobayashi, H. Yamamoto, Endothelin 1 mediates endothelial cell-dependent proliferation of vascular pericytes, Biochem. Biophys. Res. Commun. 191 (1993) 840–846.
[36] Q. Yan, E.H. Sage, Transforming growth factor-β1 induces apoptotic cell death in cultured retinal endothelial cells but not pericytes: association with decreased expression of p21waf1/cip1, J. Cell. Biochem. 70 (1998) 70–83.

ELSEVIER

Journal of the Neurological Sciences 225 (2004) 65–69

Journal of the Neurological Sciences

www.elsevier.com/locate/jns

Crossed cerebellar hypoperfusion in hyperacute ischemic stroke

Masahiro Kamouchi[a,b,*], Masatoshi Fujishima[b], Yoshisuke Saku[a], Setsuro Ibayashi[b], Mitsuo Iida[b]

[a]*Division of Cerebrovascular Disorders, St. Mary's Hospital, Kurume, Fukuoka, Japan*
[b]*Department of Medicine and Clinical Science, Graduate School of Medical Sciences, Kyushu University, Maidashi 3-1-1, Higashi-ku, Fukuoka 812-8582, Japan*

Received 28 January 2004; received in revised form 29 April 2004; accepted 2 July 2004
Available online 20 August 2004

Abstract

Objective: In chronic stage of cerebral hemispheric infarction, contralateral cerebellar blood flow and metabolism are depressed, which is known as crossed cerebellar diaschisis (CCD). The present study was performed to elucidate (1) whether the diaschisis occurs in hyperacute stage of ischemic stroke when computed tomography (CT) scans is not able to identify infarction, and (2) which site of lesion in the cerebrum is responsible for the depression in contralateral cerebellar blood flow.

Methods: Single photon emission computed tomography was performed in 21 patients with middle cerebral artery (MCA) embolic infarction within 6 h of the onset (3.2±1.1 h, mean±S.D.). Regions of interest (ROIs) were symmetrically located in the cerebral hemispheres including cerebral cortex and subcortex, and in the cerebellar hemispheres.

Results: The side-to-side ratio of cerebellar blood flow ipsilateral to that contralateral to cerebral infarct was significantly increased compared with that in normal control ($P<0.001$), indicating that contralateral cerebellar blood flow was significantly depressed. In hyperacute stage, the ratio of cerebellar blood flow appeared to be associated with the ratio of cerebral blood flow in whole hemispheres ($r=0.44$, $P<0.05$), in anterior frontal lobe ($r=0.44$, $P<0.05$) and in anterior temporal lobe ($r=0.58$, $P<0.01$), but not in infarct areas ($r=0.26$, $P=0.3$). Stepwise regression analysis revealed that the ratios in cerebellar hemispheres were associated with those in anterior temporal lobe (multiple regression analysis, $r=0.58$, $P<0.01$).

Conclusions: Crossed cerebellar diaschisis occurs at hyperacute stage of stroke of the MCA infarction. It may be related to the hypoperfusion in the anterior frontal and anterior temporal lobes of the cerebrum where regional blood flow is decreased by ischemic infarction per se or by ipsilateral hemispheric depression from infarct area (diaschisis mechanism).

Keywords: Cerebrovascular circulation; Single photon emission computed tomography; Middle cerebral artery occlusion; Diaschisis

1. Introduction

It has been known that cerebral hemispheric infarction depresses cerebellar blood flow and metabolism unrelated to the site of lesion [1–3]. A reduction of cerebellar blood flow contralateral to the supratentorial infarction has been recognized in the subacute and chronic stage of stroke. Unfortunately, few studies have been performed in the initial hours of ischemic events in humans. Moreover, the hemodynamic studies in acute stroke have not investigated on the remote effects of the infarct [4–8]. Thus, it is still unknown whether crossed cerebellar diaschisis (CCD) is present in the first few hours of ischemic stroke of the cerebrum. Moreover, there is no agreement concerning the serial changes in CCD. Most investigators have reported that CCD does not resolve [3,9,10], while others have suggested that CCD is an acute phenomenon and therefore it diminishes with time [11,12]. In contrast, there was another study demonstrating that the degree of CCD increases as the time from stroke ictus elapses [13].

* Corresponding author. Tel.: +81 92 642 5256; fax: +81 92 642 5271.
E-mail address: kamouchi@intmed2.med.kyushu-u.ac.jp (M. Kamouchi).

0022-510X/$ - see front matter © 2004 Elsevier B.V. All rights reserved.
doi:10.1016/j.jns.2004.07.004

Although CCD has been studied in stroke patients with both positron emission tomography (PET) and single photon emission computed tomography (SPECT), it is still equivocal concerning the lesion causing CCD. A PET study showed that differences in the metabolic rate and blood flow between both cerebellar hemispheres are only apparent when the cerebral infarct involves the frontal lobe [9]. In animal models, it has been reported that CCD is a response to reduced afferent input from interconnected brain regions, especially the contralateral frontal cortex [14]. However, little is known concerning CCD at hyperacute stage of cerebral infarction in humans.

In the present study, cerebral and cerebellar blood flows were evaluated in cerebral infarction within 6 h of the onset with SPECT. The aim of the present study is to elucidate whether CCD occurs at the hyperacute stage of the ischemic insult and which site of the lesion most affects the reduction of blood flow in contralateral cerebellar hemisphere.

2. Subjects and methods

Patients with acute unilateral middle cerebral artery (MCA) infarction were prospectively recruited for this study from the St. Mary's Hospital. We investigated 21 patients who had first-ever MCA infarction and underwent SPECT within 6 h of the onset. Patients ranged in age from 45 to 86 years (67±13 years, mean±S.D.) and included 12 females. All patients were admitted with the clinical diagnosis of acute embolism in MCA territory, although CT scans on admission did not show any infarction in the territory yet. Follow-up CT was performed within 2 days after onset and revealed infarcts in the territory of MCA, including cortical infarct in three patients, deep structure infarct in one, cortical and deep structure infarct in 10, and whole MCA territory infarct in seven.

SPECT using ^{99m}Tc-HMPAO (555–925 mBq) was carried out with a rotating gamma camera (Shimadzu, Japan). The tracer was administered within 6 h of the onset (3.2±1.1 h). Follow-up SPECT was repeated in 13 patients at 3–7 days after the onset. Data were reconstructed to obtain consecutive axial slices every 12 mm parallel to and above the orbitomeatal line. Symmetrical regions of interest (ROIs) were set at whole cerebral hemisphere and cerebellar hemisphere, and also in six cerebral cortical regions; anterior and posterior frontal, anterior and posterior temporal, parietal and occipital lobe as well as two subcortical regions; basal ganglia and thalamus (Fig. 1). The size of ROI was 2×2. ROIs were additionally set at infarct lesion corresponding to the area on CT in the chronic stage by visual guidance. The linearization correction was done according to the methods reported by Lassen et al. [15]. In each ROI, the difference in total counts in both sides was expressed as a ratio of the values of the affected side to the non-affected side in the cerebral hemispheres, and as a ratio of the values ipsilateral to contralateral to the cerebral infarct in the cerebellar hemispheres. Asymmetry index was also used for correlation analysis. The asymmetry index was calculated as the difference between hemispheres as a percentage of the mean: asymmetry index=$(I-C)/(I+C)\times 200\%$, where I and C refer to the maximal cerebral count value on the side ipsilateral to the infarct and that on the contralateral side, respectively.

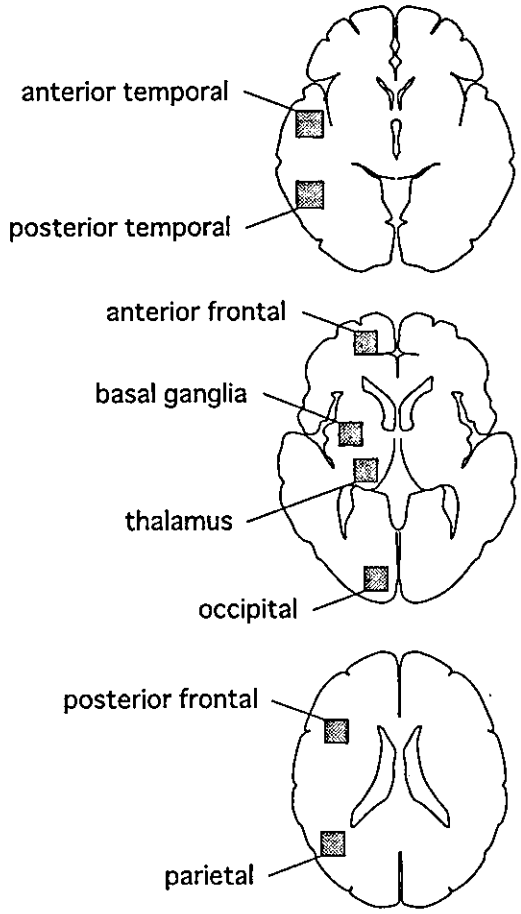

Fig. 1. The location of ROIs. The size of the ROI was 2×2 cm and its location is shown in the figure. ROI was also set at most marked hypoperfusion area within the infarct area by visual guidance.

The values observed in those, who never had history of cerebrovascular disease, and also had no brain lesion on CT scan, were adopted as normal control. Fifty-one controls (28 female) were from 43 to 79 years of age (67±7 years), which was not different from that in patients group. We analyzed the difference in the side-to-side ratio in each ROI using t-test. Linear regression analysis was performed to examine relationship between the side-to-side ratios in each ROI. Multiple regression analysis was performed to examine the possible association of the ratio or asymmetry index in various regions with that in cerebellar hemisphere. Regression models included the

Table 1
Side-to-side ratio of blood flow in cerebral and cerebellar hemispheres

ROI	Ratio (mean±S.D.)
Whole hemisphere	0.87±0.13
Infarct areas	0.65±0.18
Frontal lobe (anterior)	0.93±0.06
Frontal lobe (posterior)	0.81±0.30
Temporal lobe (anterior)	0.81±0.25
Temporal lobe (posterior)	0.77±0.21
Parietal lobe	0.84±0.19
Occipital lobe	0.96±0.07
Thalamus	0.93±0.09
Basal ganglia	0.98±0.40
Cerebellar hemisphere	1.04±0.04

The ratio of cerebral hemispheres and infarct areas below 1.0 indicates the decreased cerebral blood flow in the affected hemispheres or infarct areas. The ratio of cerebellar hemispheres above 1.0 indicates the decreased cerebellar blood flow contralateral to infarct (crossed cerebellar diaschisis).

potential predictive variables. These variables are obtained in all regions in MCA territory. A P value less than 0.05 was considered to be significant. The values were expressed as the mean±S.D.

3. Results

3.1. Cerebellar blood flow in hyperacute ischemic stroke

The side-to-side ratio of blood flow in cerebellar hemispheres within 6 h after the onset was significantly high (1.04±0.04, n=21) compared with that seen in control (1.00±0.04, n=51, unpaired t-test P<0.001), indicating that cerebellar blood flow contralateral to the infarct was decreased in the patients, namely crossed cerebellar diaschisis. Two patients had cerebellar values of 1.09 and 1.11, both of which were outside the 95% confidence interval (0.93–1.07) of those calculated on controls. The average ratios in whole cerebral hemispheres and in infarct areas which were identified on CT scan at chronic stage were 0.87±0.13 and 0.65±0.18, respectively (Table 1), indicating that cerebral blood flow was decreased in the affected hemisphere or in the infarct areas. Among the 13 patients in which follow-up SPECT image was available at 3–7 days after the onset, the ratio in the cerebellar hemispheres remained high in follow-up study (within 6 h, 1.03±0.04, follow-up image, 1.05±0.07, paired t-test, P=0.2), suggesting the hypoperfusion to be continued.

3.2. Relationship between cerebral blood flow in various regions and cerebellar blood flow

The side-to-side ratios of blood flow in cerebellar hemispheres did not correlate with the ratios in infarct areas (linear regression, r=0.26, P=0.3), but they were associated with the ratios in whole cerebral hemispheres (r=0.44, P<0.05). The ratios in infarct area was associated with those in whole cerebral hemisphere (r=0.73, P<0.0005) as well as in the MCA territory including posterior frontal (r=0.66, P<0.005), anterior temporal (r=0.55, P<0.05), posterior temporal (r=0.60, P<0.005), and parietal (r=0.52, P<0.05) lobes, but not with those in anterior frontal (r=0.34, P=0.1), occipital (r=0.27, P=0.2) lobes, thalamus (r=0.28, P=0.2), and basal ganglia (r=0.31, P=0.2).

To examine which area most affects the contralateral cerebellar blood flow, we then analyzed the relationship of the ratios of blood flow between various cerebral hemisphere and cerebellar hemispheres (Table 2). Linear regression analysis showed that the ratios in cerebellar hemispheres seemed to be associated with those in the anterior frontal (r=0.44, P<0.05) and anterior temporal lobe of cerebral hemispheres (r=0.58, P<0.01, Fig. 2). No significant correlations could be detected in the other cortical (posterior frontal, temporal, parietal, and occipital lobes) and subcortical areas (thalamus and basal ganglia). Stepwise regression analysis revealed that the ratios in cerebellar hemispheres were only associated with those in anterior temporal lobe (multiple regression analysis, r=0.58, P<0.01). When the asymmetry index was adopted as variables instead of the side-to-side ratios, linear and stepwise regression analyses showed the same results

Table 2
Correlation of the side-to-side ratio of cerebral hemispheric blood flow with the ratio of cerebellar blood flow

ROI	Ratio	r	Regression coefficient 95% CI	P
Whole hemisphere	0.59 to 1.01	0.44	−0.283 to −0.002	<0.05
Infarct areas	0.29 to 0.92	0.26	−0.161 to 0.047	0.3
Frontal lobe (anterior)	0.80 to 1.06	0.44	−0.550 to −0.006	<0.05
Frontal lobe (posterior)	0.32 to 1.4	0.38	−0.113 to 0.009	0.09
Temporal lobe (anterior)	0.29 to 1.38	0.58	−0.159 to −0.031	<0.01
Temporal lobe (posterior)	0.26 to 1.02	0.32	−0.150 to 0.026	0.2
Parietal lobe	0.40 to 1.11	0.29	−0.162 to 0.038	0.2
Occipital lobe	0.80 to 1.07	0.08	−0.313 to 0.219	0.7
Thalamus	0.62 to 1.11	0.11	−0.168 to 0.267	0.6
Basal ganglia	0.58 to 2.56	0.30	−0.016 to 0.077	0.2

Linear regression analysis was performed to examine the correlation between cerebral blood flow in each supratentorial region and cerebellar blood flow.

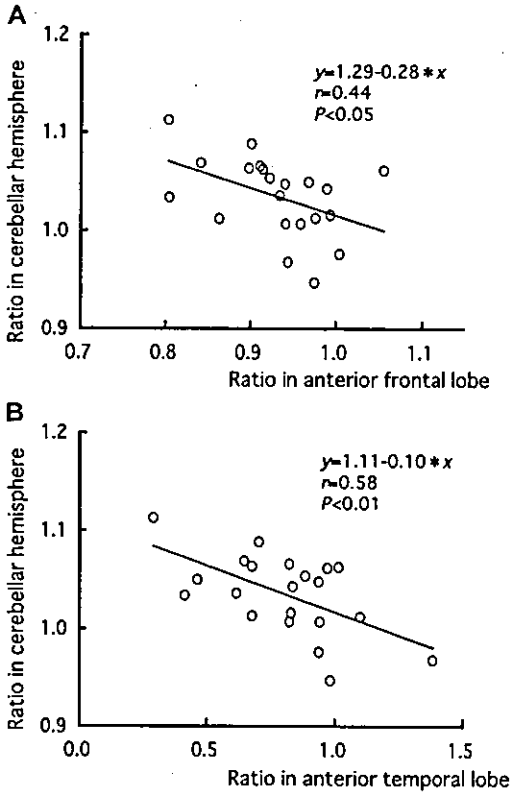

Fig. 2. Correlation between the ratios in cerebellar hemispheres and those in anterior frontal (A) and anterior temporal lobe (B). Line was drawn based on linear regression equation. Ratio indicates the side-to-side ratio of the RI counts in each region.

concerning the correlation of blood flow between the various cerebral hemispheres and cerebellar hemispheres.

4. Discussion

Supratentorial ischemic strokes cause the depression in blood flow and metabolism in the contralateral cerebellum, which was first demonstrated by Baron and coworkers [2,16] with PET in 1980. The mechanism responsible for CCD is thought to be deafferentiation through the cortico–ponto–cerebellar tract [16]. Recent reports postulated that diaschisis may play a role in stroke recovery, although it is still controversial [17–21]. Data concerning the period when CCD emerges in ischemic stroke are still lacking. In rat model, focal cerebral ischemia caused by occlusion of the MCA and common carotid artery induced a rapid decrease in neuronal activity and blood flow in contralateral cerebellum [14]. In baboons, contralateral cerebellar diaschisis was caused by functional deactivation at early stage of cerebral infarction [22]. Eckard et al. [23] reported a case of CCD during temporary balloon occlusion of the internal carotid artery. In the present study, we performed SPECT in patients with cerebral embolism within 6 h (3.2±1.1 h, mean±SD) of the onset when CT did not show any evident change as yet, and found that CCD occurred in superacute stage irrespective of CT change, suggesting that contralateral cerebellar diaschisis is a rapid response to cerebral ischemia.

There appear to be two advantages in the assessment of cerebral blood flow at hyperacute stage. Our previous study showed that a high distribution of ^{99m}Tc-HMPAO in infarct areas occurs frequently and transiently in the subacute stage of cerebral embolism [24]. Therefore, to investigate possible association between supratentorial lesion and CCD, SPECT should be done before postischemic hyperfixation occurs. In the present study, however, detailed observations revealed that the side-to-side ratio of hemispheric blood flow partially exceeded 1.0 in 3 patients, indicating that postischemic hyperfixation potentially occurs in some lesion even at hyperacute stage, probably due to spontaneous recanalization of the occluded MCA. Secondly, neuronal activity may be depressed in parallel in the lesion where hypoperfusion is severe at hyperacute stage. PET analysis will provide further information of blood flow and metabolism, however it is difficult to perform the test at hyperacute phase. As a result, PET data within few hours from the onset have not been available. In contrast, SPECT is possible to measure blood flow in the hyperacute stage, and this technique is potentially useful to investigate the mechanisms of CCD.

PET study in chronic stage of cerebral hemispheric infarction showed that differences in blood flow and metabolism between both cerebellar hemispheres were significant when the infarct involved the frontal lobe [9]. Pantano et al. [3] demonstrated that CCD was more prominent when the supratentorial infarct involved the internal capsule or the cortical mantle extensively. They also suggested that destruction of the pyramidal tract is neither necessary nor sufficient to induce CCD. In rat model, Gold and Lauritzen [14] showed that decreases of activity involving the frontal cortex produced the largest decrease in contralateral cerebellar electrical activity and blood flow. Kim et al. [25] reported that the location rather than the extent or severity of the lesion may be the major determinant for the occurrence and magnitude of CCD in patients with cerebral infarction. In the present study, contralateral cerebellar blood flow may be associated with the blood flow in anterior frontal lobe which was independent of the severity of the hypoperfusion in infarct area. Moreover, it was also significantly associated with anterior temporal lobe but not other regions in the territory of MCA. Stepwise regression analysis revealed the significant association between the contralateral cerebellar hypoperfusion and blood flow reduction in anterior temporal lobe. Therefore, CCD may not be related to the severity of hypoperfusion in infarct area but the decreased blood flow in supratentorial specific areas. There may be following possibilities for the mechanisms in hyperacute stage: (1) an interconnected tract between supratentorial cortex and contralateral cerebellar hemisphere was disrupted by the

hypoperfusion in the MCA territory; (2) the hypoperfusion in the MCA territory depressed the contralateral cerebellar activity via anterior frontal lobe. In the animal model, the degree of depressed neuronal activity is determined by the extent of hypoperfusion in the lesions [14]. Thus, we concluded that CCD, namely the depression of contralateral cerebellar blood flow, is related to the depressed activity in supratentorial specific areas including anterior frontal or anterior temporal lobe where regional blood flow is decreased by ischemic infarction per se or by ipsilateral hemispheric depression from infarct area (diaschisis mechanism). Association between CCD and lesion in frontal lobe has been reported so far, whereas association with that in temporal lobe has not been reported. Moreover, ROIs may not have been set exactly on the dying cortex or surrounding viable cortex in the present study because of methodological limitation. To clarify the mechanism, clinical study using magnetic resonance imaging in superacute stage of infarction will be possible and available, or experimental study using ischemic animal model is needed.

References

[1] Baron JC, Bousser MG, Comar D, Castaigne P. 'Crossed cerebellar diaschisis' in human supratentorial brain infarction. Trans Am Neurol Ass 1980;105:459–61.

[2] Baron JC, Rougemont D, Soussaline F, Bustany P, Crouzel C, Bousser MG, et al. Local interrelationships of cerebral oxygen consumption and glucose utilization in normal subjects and in ischemic stroke patients: a positron tomography study. J Cereb Blood Flow Metab 1984;4(2):140–9.

[3] Pantano P, Baron JC, Samson Y, Bousser MG, Derouesne C, Comar D. Crossed cerebellar diaschisis. Further studies. Brain 1986; 109(Pt. 4):677–94.

[4] Alexandrov AV, Bladin CF, Ehrlich LE, Norris JW. Noninvasive assessment of intracranial perfusion in acute cerebral ischemia. J Neuroimaging 1995;5(2):76–82.

[5] Giubilei F, Lenzi GL, Di Piero V, Pozzilli C, Pantano P, Bastianello S, et al. Predictive value of brain perfusion single-photon emission computed tomography in acute ischemic stroke. Stroke 1990;21(6): 895–900.

[6] Firlik AD, Kaufmann AM, Wechsler LR, Firlik KS, Fukui MB, Yonas H. Quantitative cerebral blood flow determinations in acute ischemic stroke. Relationship to computed tomography and angiography. Stroke 1997;28(11):2208–13.

[7] Hanson SK, Grotta JC, Rhoades H, Tran HD, Lamki LM, Barron BJ, et al. Value of single-photon emission-computed tomography in acute stroke therapeutic trials. Stroke 1993;24(9):1322–9.

[8] Shimosegawa E, Hatazawa J, Inugami A, Fujita H, Ogawa T, Aizawa Y, et al. Cerebral infarction within six hours of onset: prediction of completed infarction with technetium-99m-HMPAO SPECT. J Nucl Med 1994;35(7):1097–103.

[9] Martin WR, Raichle ME. Cerebellar blood flow and metabolism in cerebral hemisphere infarction. Ann Neurol 1983;14(2):168–76.

[10] Meneghetti G, Vorstrup S, Mickey B, Lindewald H, Lassen NA. Crossed cerebellar diaschisis in ischemic stroke: a study of regional cerebral blood flow by ^{133}Xe inhalation and single photon emission computerized tomography. J Cereb Blood Flow Metab 1984;4(2): 235–40.

[11] Kushner M, Alavi A, Reivich M, Dann R, Burke A, Robinson G. Contralateral cerebellar hypometabolism following cerebral insult: a positron emission tomographic study. Ann Neurol 1984;15(5):425–34.

[12] Pantano P, Lenzi GL, Guidetti B, Di Piero V, Gerundini P, Savi AR, et al. Crossed cerebellar diaschisis in patients with cerebral ischemia assessed by SPECT and ^{123}I-HIPDM. Eur Neurol 1987;27(3):142–8.

[13] Lenzi GL, Frackowiak RS, Jones T. Cerebral oxygen metabolism and blood flow in human cerebral ischemic infarction. J Cereb Blood Flow Metab 1982;2(3):321–35.

[14] Gold L, Lauritzen M. Neuronal deactivation explains decreased cerebellar blood flow in response to focal cerebral ischemia or suppressed neocortical function. Proc Natl Acad Sci U S A 2002;99(11):7699–704.

[15] Lassen NA, Andersen AR, Friberg L, Paulson OB. The retention of [^{99m}Tc]-D,L-HM-PAO in the human brain after intracarotid bolus injection: a kinetic analysis. J Cereb Blood Flow Metab 1988;8 (6):S13.

[16] Feeney DM, Baron JC. Diaschisis. Stroke 1986;17(5):817–30.

[17] Pantano P, Formisano R, Ricci M, Di Piero V, Sabatini U, Di Pofi B, et al. Motor recovery after stroke. Morphological and functional brain alterations. Brain 1996;119(Pt. 6):1849–57.

[18] Iglesias S, Marchal G, Rioux P, Beaudouin V, Hauttement AJ, de la Sayette V. Do changes in oxygen metabolism in the unaffected cerebral hemisphere underlie early neurological recovery after stroke? A positron emission tomography study. Stroke 1996;27(7): 1192–9.

[19] Iglesias S, Marchal G, Viader F. Baron JC: Delayed intrahemispheric remote hypometabolism. Correlations with early recovery after stroke. Cerebrovasc Dis 2000;10(5):391–402.

[20] Infeld B, Davis SM, Lichtenstein M, Mitchell PJ, Hopper JL. Crossed cerebellar diaschisis and brain recovery after stroke. Stroke 1995;26(1):90–5.

[21] Seitz RJ, Azari NP, Knorr U, Binkofski F, Herzog H, Freund HJ. The role of diaschisis in stroke recovery. Stroke 1999;30(9):1844–50.

[22] Dettmers C, Hartmann A, Rommel T, Hartmann S, Pappata S, Baron JC. Contralateral cerebellar diaschisis 7 hours after MCA-occlusion in primates. Neurol Res 1995;17(2):109–12.

[23] Eckard DA, Purdy PD, Bonte F. Crossed cerebellar diaschisis and loss of consciousness during temporary balloon occlusion of the internal carotid artery. AJNR Am J Neuroradiol 1992;13(1):55–7.

[24] Kamouchi M, Saku Y, Ibayashi S, Katsuragi M, Sadoshima S, Fujishima M. Changes in the cerebral and cerebellar blood flow in cerebral embolism. Cerebrovasc Dis 1996;6(5):301–7.

[25] Kim SE, Choi CW, Yoon BW, Chung JK, Roh JH, Lee MC, et al. Crossed-cerebellar diaschisis in cerebral infarction: technetium-99m-HMPAO SPECT and MRI. J Nucl Med 1997;38(1):14–9.

Original Paper

Cerebrovascular Diseases

Cerebrovasc Dis 2004;17:98–105
DOI: 10.1159/000075776

Received: September 20, 2002
Accepted: June 2, 2003
Published online: December 23, 2003

Incidence, Etiology, and Outcome of Stroke in Patients on Continuous Ambulatory Peritoneal Dialysis

Kazunori Toyoda[a] Kenichiro Fujii[a] Takashi Ando[b] Yasuhiro Kumai[a]
Setsuro Ibayashi[c] Mitsuo Iida[c]

[a]Stroke Center and [b]Kidney Center, Fukuoka Red Cross Hospital, and [c]Department of Medicine and Clinical Science, Graduate School of Medical Sciences, Kyushu University, Fukuoka, Japan

Key Words
End-stage renal disease · Stroke · Cerebrovascular disorders · Peritoneal dialysis · Hemodialysis

Abstract
Background: Little information exists on clinical features of stroke in patients receiving continuous ambulatory peritoneal dialysis (CAPD). The goals of this study was to clarify features of stroke in CAPD patients, to determine factors to predict onset of stroke during chronic CAPD, and to determine whether CAPD had an advantage over hemodialysis (HD) for prevention of stroke. ***Methods:*** We determined features of stroke in 12 patients (14 attacks including 7 parenchymal and 1 subarachnoid hemorrhage and 6 infarction) among 188 consecutive patients on CAPD, and compared them with those of 137 stroke patients among 1,681 consecutive patients on hemodialysis. ***Results:*** Incidence of stroke for CAPD patients (15.7 per 1,000 person-years) was high compared with that of HD patients (approximately 12) or general residents in our suburban town. Patients with stroke on CAPD were younger than those on HD (52 ± 12 vs. 62 ± 11 years, $p = 0.008$). Mean arterial pressure (MAP) of patients with stroke increased after the introduction of CAPD ($p = 0.01$), whereas that of patients without stroke did not change. Increase in MAP during chronic CAPD was related independently to the occurrence of total stroke or brain hemorrhage. The majority of CAPD patients with stroke (67%) were dead or dependent in the chronic stage of stroke. ***Conclusion:*** CAPD patients seem to have a greater risk of stroke than the general population primarily because of poor control of hypertension, presumably in part due to overhydration. CAPD does not seem to have an advantage over HD for the prevention of stroke.

Introduction

Continuous ambulatory peritoneal dialysis (CAPD) is in widespread use for the home-based renal replacement therapy of end-stage renal disease. In this strategy, dialysate is manually infused into the peritoneal cavity via a chronic peritoneal catheter and exchanged usually 4 times a day. Approximately half of patients with end-stage renal disease receive CAPD in the United Kingdom and New Zealand, one third in Australia and Canada, and approximately 10% in the United States [1]. The wide discrepancy of the prevalence of CAPD among countries seems to result from nonmedical factors including economic and geographic problems [2]. Japan has 1,465 patients with

KARGER
Fax + 41 61 306 12 34
E-Mail karger@karger.ch
www.karger.com

1015–9770/04/0173–0098$21.00/0

Accessible online at:
www.karger.com/ced

Kazunori Toyoda, MD
Department of Cerebrovascular Disease, National Kyushu Medical Center
1-8-1 Jigyohama, Chuo-ku
Fukuoka 810-8563 (Japan)
Tel. +81 92 852 0700, Fax +81 92 846 8485, E-Mail toyoda@qmed.hosp.go.jp

end-stage renal disease per million population, the highest prevalent rates in the world, and about 5% of them receive CAPD [1].

Stroke is the second or third leading cause of death in patients on CAPD next to cardiac diseases, accounting for about 10% of deaths during CAPD [3–5]. CAPD has been considered to be superior to hemodialysis (HD) for cardiovascular and cerebrovascular protection, because CAPD was reported to keep better control of hypertension [6, 7]. Recently, long duration of CAPD, however, has been reported to be disadvantageous to cardiac function compared with HD, possibly because of the development of hypervolemia [8]. Thus, it is in dispute which dialysis has an advantage for the prevention of stroke. To resolve this question, detailed analysis for patients on CAPD with stroke, such as of the type of stroke and alteration of blood pressure, is necessary.

Our clinic has monitored all patients who had started CAPD in the Kidney Center since 1980. The first goal of this study was to clarify clinical features of stroke in CAPD patients, and to determine factors to predict the onset of stroke during chronic CAPD. The second goal was to determine whether CAPD had an advantage over HD for the prevention of stroke.

Patients and Methods

From May 1980 to October 2001, 188 patients started CAPD and 1,681 started HD in our Kidney Center. The choice between CAPD and HD depended on each patient's desire in principle, except for some contraindications to CAPD, including documented loss of peritoneal function or extensive abdominal adhesions, patients being physically or mentally incapable of performing CAPD in the absence of a suitable assistant, and uncorrectable mechanical defects that prevent effective CAPD like surgically irreparable hernia [9]. In addition, we often recommended HD, not CAPD, to patients over 70 years of age because they might have troubles to perform the exchange of dialysate by themselves, and to patients with diabetes because glucose loading via dialysate might worsen glucose tolerance. Because residual kidney function contributes significantly to total solute and water removal during the first few years of CAPD therapy, we often introduced CAPD while patients still kept somewhat good kidney function.

Among 188 patients on CAPD, we identified patients who developed stroke while they received CAPD. To assess indicators for the occurrence of stroke, clinical characteristics at initiation of CAPD and during chronic CAPD listed in table 1 were analyzed for all the patients with or without stroke. Characteristics during chronic CAPD were evaluated after 4 years of CAPD, or at the last day in the outpatient clinic if duration of CAPD (before the onset of stroke) was less than 4 years. Blood urea nitrogen, serum creatinine, and mean arterial pressure (MAP) were measured by averaging 3 consecutive data at the clinic every 2–4 weeks. Residual renal urea clearance normalized to total body water, K_t/V_{urea}, was measured to evaluate the quality of dialysis. The maximal cardiac diameter divided by the maximal internal thoracic diameter, i.e. cardiothoracic ratio, was measured on the chest roentgenogram at the standing position. For patients with stroke, the type and etiology of their strokes were assessed according to the classification of cerebrovascular diseases III by NINDS [10].

The advantage of CAPD over HD for the prevention of stroke was tested as follows. First, to determine selection bias between patients with CAPD and HD, we examined baseline characteristics of the patients at initiation of HD; age, sex, and original kidney diseases for all 1,681 patients who started HD in our Kidney Center, and duration of renal insufficiency, blood urea nitrogen, serum creatinine, and MAP for 200 among the 1,681 patients selected at random. Second, we examined 137 consecutive HD patients who developed acute stroke and were hospitalized in our institute among the 1,681 patients and compared their clinical characteristics at initiation of dialysis and during chronic dialysis with those of CAPD patients with stroke. Third, to assess the prevalence of young-onset stroke during dialysis, we analyzed the incidence of stroke within 10 years after initiation of the dialysis therapy in patients who had started CAPD or HD under 45 years of age. Finally, we determined clinical severity of stroke for patients on CAPD or HD. Neurological deficits on admission were evaluated using the National Institute of Health Stroke Scale (NIHSS). Functional outcome 8 weeks after stroke onset was evaluated using the Barthel Index. Patients with a Barthel Index score < 50 were regarded as dependent. For 3 patients on CAPD and 34 patients on HD who developed stroke before 1993, NIHSS and the Barthel Index were assessed afterwards based on their medical records. NIHSS seems to be abstracted from medical records with a high degree of reliability and validity for the purposes of retrospective studies of acute stroke outcome [11].

Values are expressed as mean ± SD. Student's t test and χ^2 test were used as univariate analysis. Multivariate analysis was performed by logistic regression using the significant factors. $p < 0.05$ was accepted as statistically significant.

Results

Features of Stroke for Patients on CAPD

We enrolled 188 patients on CAPD, 126 men and 62 women, aged 46 ± 14 years. The duration of observation was 892.9 person-years. Twelve patients developed stroke in total 14 times; 6 brain infarction, 7 brain hemorrhage, and 1 subarachnoid hemorrhage (table 2). One patient (patient 6) developed brain hemorrhage 13 months after brain infarction. Another patient (patient 11) suffered brain hemorrhage twice at an interval of 9 days. The incidences of total stroke, brain infarction, brain hemorrhage, and subarachnoid hemorrhage were 15.7, 6.7, 7.8, and 1.1 per 1,000 person-years, respectively.

Brain infarction consisted of 2 atherothrombotic, 3 lacunar, and 1 cardioembolic infarction. Infarcts were located in the frontal cortex, parietal subcortex, basal ganglia, putamen, and pons (2 patients). All patients with

Table 1. Characteristics of patients

Variable	CAPD		p value CAPD-S (–) vs. CAPD-S (+)	HD	p value CAPD-S (+) vs. HD-S (+)
	stroke (–) (n = 176)	stroke (+) (n = 12)		stroke (+) (n = 137)	
Baseline characteristics at initiation of dialysis					
Age, years	46 ± 14	48 ± 12	NS	55 ± 13	NS (0.06)
Duration of renal disease, years	13.2 ± 8.5	11.5 ± 8.3	NS	–	–
Male sex, %	66	75	NS	65	NS
Blood urea nitrogen, mg/dl	85.8 ± 24.2	73.3 ± 22.5	NS	–	–
Serum creatinine, mg/dl	9.9 ± 2.9	9.9 ± 2.8	NS	–	–
MAP, mm Hg	107 ± 15	103 ± 8	NS	–	–
Original kidney disease, %			NS		0.003
Chronic glomerulonephritis	70	75		25	
Diabetic nephropathy	11	17		42	
Hypertensive nephrosclerosis	5	0		17	
Lupus nephritis	2	8		1	
Polycystic kidney disease	1	0		2	
Others	11	0		13	
Characteristics during chronic dialysis (before onset of stroke)					
Duration of dialysis, years	4.7 ± 3.5	4.6 ± 3.5[a]	NS	6.7 ± 5.8[a]	NS
Hypertension, %	81	92	NS	85	NS
Diabetes, %	21	33	NS	48	NS
Dyslipidemia, %	25	33	NS	13	NS
Atrial fibrillation, %	5	17	NS	14	NS
Ischemic heart disease, %	12	25	NS	13	NS
K_t/V_{urea}	2.19 ± 0.16	2.17 ± 0.32	NS	–	–
MAP, mm Hg	107 ± 14	115 ± 16	0.05	–	–
ΔMAP[b], mm Hg	0 ± 13	13 ± 15	0.002	–	–
Cardiothoracic ratio, %	46.9 ± 4.9	50.0 ± 3.8	0.04	–	–
Medication					
Antihypertensives, %	76	83	NS	–	–
Antihypertensives, n of agents	1.3 ± 0.9	1.4 ± 1.2	NS		–
Aspirin, %	9	0	NS	–	–
Warfarin, %	2	0	NS	–	–
Characteristics on stroke					
Age at stroke onset, years	–	52 ± 12	–	62 ± 11	0.008
Type of stroke, %			–		NS
Brain infarction	–	43		58	
Brain hemorrhage	–	50		38	
Subarachnoid hemorrhage	–	7		4	
Subtype of brain infarction, %			–		NS
Atherothrombotic	–	33		25	
Lacunar	–	50		48	
Cardioembolic	–	17		27	
NIH-SS at admission, %			–		NS
0–6	–	42		49	
7–15	–	17		24	
16–42	–	42		27	
Dead or dependent (Barthel Index ≤ 50) at discharge, %	–	67		43	NS (0.10)

[a] Until stroke onset.
[b] Increase in MAP during chronic CAPD compared with initiation of CAPD (mean ± SD).

Table 2. Characteristics of stroke patients on CAPD

Patient No.	Age[1]	Sex	Original kidney disease	Risk factors	Antihypertensives	Profiles of stroke				
						type	etiology	location	NIHSS[1]	prognosis[2]
1	59	m	CGN	HT, DL, IHD	Ca (2 agents)	BI	atherothrombotic	subcortex	12	ID
2	61	f	CGN	HT, DL	Ca	BI	atherothrombotic	cortex	2	100
3	70	m	CGN	HT, DM, af, IHD	Ca	BI	cardioembolic	basal ganglia	10	ID
4	34	f	CGN	HT	Ca, β	BI	lacunar	pons	2	100
5	65	m	CGN	HT, IHD	none	BI	lacunar	pons	5	ID
6-i	39	m	CGN	HT, DL	Ca, ACEI	BI	lacunar	putamen	1	100
6-ii	40	m				BH	HT	putamen	>16	DD
7	54	m	diabetic	HT, DM, DL, af	Ca, ACEI	BH	HT	thalamus	4	90
8	49	f	lupus	HT	β	BH	HT, (vasculitis)	putamen	>16	35
9	44	m	diabetic	HT, DM	Ca	BH	HT	pons	>16	DD
10	48	m	CGN	HT	Ca, ACEI, β	BH	HT	putamen	>16	DD
11-i	40	m	CGN	HT	Ca, α	BH	HT	thalamus	1	100
11-ii	40	m				BH	HT	putamen	4	100
12	68	m	CGN	DM, LD	none	SAH	unknown	–	>16	ID

Patient 6 developed brain hemorrhage 13 months after brain infarction. Patient 11 suffered brain hemorrhage twice at an interval of 9 days. CGN = Chronic glomerulonephritis; HT = hypertension; DM = diabetes mellitus; DL = dyslipidemia; IHD = ischemic heart disease; af = atrial fibrillation; Ca = calcium channel blocker; α = α blocker; β = β blocker; ACEI = angiotensin-converting enzyme inhibitor; BI = brain infarction; BH = brain hemorrhage; SAH = subarachnoid hemorrhage; ID = indirect death; DD = direct death.

[1] At the onset of stroke.

[2] Number indicates Barthel Index scores 8 weeks after stroke onset.

brain hemorrhage were hypertensive, with possible lupus vasculitis in 1 patient with systemic lupus erythematosus. Hematomas were distributed in the putamen in 4 patients, in the thalamus in 2, and in the pons in 1 patient. The cause of subarachnoid hemorrhage was unknown.

Comparison between CAPD Patients with and without Stroke

Clinical characteristics at initiation of CAPD were similar between CAPD patients with and without stroke (table 1). Among the characteristics during chronic CAPD, the cardiothoracic ratio in patients with stroke was greater than that without stroke ($p = 0.04$). MAP of chronic CAPD patients with stroke increased from 103 ± 8 mm Hg at the initiation of CAPD to 115 ± 16 mm Hg in the chronic stage ($p = 0.01$), whereas that of CAPD patients without stroke did not change (107 ± 15 to 107 ± 14 mm Hg; fig. 1). Increase in MAP in patients with stroke during chronic CAPD was greater than that in patients without stroke ($p = 0.002$). There were no differences, however, in the use of antihypertensives between patients with and without stroke. As antithrombotic agents, aspirin or warfarin were used for a few patients without stroke and none for patients with stroke. For patients with high blood pressure, we often used 2.5% glucose dialysate as hypertonic CAPD solution. For 10 among 12 patients with stroke (except for patients 4 and 7), we used the dialysate 1–3 times out of 4 times exchange per day according to the severity of hypertension.

After the multivariate analysis using the cardiothoracic ratio and increase in MAP as independent variables among all characteristics at initiation of CAPD and during chronic CAPD, increase in MAP alone was an independent indicator for the occurrence of stroke (odds ratio for an increase in 10 mm Hg = 2.04, 95% CI 1.21–3.43). In CAPD patients with brain hemorrhage, MAP increased from 105 ± 8 mm Hg at the initiation of CAPD to 128 ± 5 mm Hg during chronic CAPD ($p = 0.003$), and was an independent indicator for the occurrence of brain hemorrhage (odds ratio for an increase in 10 mm Hg = 5.05, 95% CI 1.94–13.12). In CAPD patients with brain infarction, MAP changed from 101 ± 9 to 111 ± 16 mm Hg ($p = 0.18$). Among them, MAP for 3 patients with lacunar infarction changed from 96 ± 6 to 118 ± 15 mm Hg ($p = 0.07$).

Comparison between Patients on CAPD and HD

In our institute, patients initiated HD (52 ± 18 years) at an older age than CAPD (46 ± 14 years, $p < 0.0001$). Male patients tended to be less frequent for HD (60%) than CAPD (67%, $p < 0.08$). The prevalence of major original kidney diseases, i.e. chronic glomerulonephritis (39%), diabetes (31%), and hypertensive nephrosclerosis